processes

MDPI

Article

Structural Changes of the Interface Material of Scallop Adductor under Ultra-High Pressure

Xue Gong [1,2], Jiang Chang [3], Yinglei Zhang [1], Danting Li [1], Ning Xia [2], Jing Wang [1] and Zhihui Sun [4,*]

[1] Light Industry College, Harbin University of Commerce, Harbin 150028, China
[2] College of Food Science, Northeast Agricultural University, Harbin 150030, China
[3] School of Food Engineering, Harbin University of Commerce, Harbin 150028, China
[4] Higher Education Development Center, Harbin University of Commerce, Harbin 150028, China
* Correspondence: sunzhihui1962@163.com

Abstract: Because of their high nutritional value, the demand for scallops is increasing year by year. In the process of improving people's living standards, the ready-to-eat characteristics and dry sales characteristics of this product make its shelling process particularly important in the production process. However, the mechanism of ultra-high pressure shelling has not yet been clarified. Therefore, in-depth study of the structural change of the scallop connection interface is of vital importance to explore the mechanism of ultra-high pressure shelling and the development of intelligent equipment from the mechanical point of view. The obturator muscle fibers and the inner surface materials of the shell at the obturator muscle scar of the scallop at 100, 200 and 300 MPa were obtained for Raman spectrum, Fourier-transform infrared spectrum and scanning electron microscopy analysis. The results showed that under the pressure of 200 MPa, the degree of protein denaturation of scallop adductor muscle increased, the elasticity disappeared, and the fiber was stretched; The deformation of the organic plasma membrane connected by the inorganic–organic interface weakens the binding force of the interface material and increases the possibility of the composite interface failure. To sum up, ultra-high pressure can effectively weaken the interface adhesion of scallop organic-inorganic composite materials, and is one of the effective ways of shelling. The research results can provide a basis for the in-depth analysis of ultra-high pressure mechanisms and the development of intelligent equipment, and provide technical support for the realization of ultra-high-pressure industrial production.

Keywords: scallop; ultra-high pressure; adductor muscle; shell; composite materials; structural changes

Citation: Gong, X.; Chang, J.; Zhang, Y.; Li, D.; Xia, N.; Wang, J.; Sun, Z. Structural Changes of the Interface Material of Scallop Adductor under Ultra-High Pressure. *Processes* **2023**, *11*, 521. https://doi.org/10.3390/pr11020521

Academic Editor: Antonino Recca

Received: 20 December 2022
Revised: 2 February 2023
Accepted: 6 February 2023
Published: 8 February 2023

1. Introduction

The scallop is a member of *Pectinidae*, *Anisomyaria*, *Lamellibranchia* and *Mollusca*, and constitutes one of the main shellfishes cultivated in coastal regions in China. Total scallop production in China in 2019 was 1.8 million metric tons (t) [1,2]. The shell and nacre of scallops are characterized by high value in use, and its meat, especially the adductor muscle (dried scallop) is known for its delicious and savory tastes, and abundant nutrients needed by human bodies [3–5], such as amino acids and micro-elements [6,7]. As people's living standards increase, an increasing number of consumers prefer scallops [8,9]. As an economically important marine-cultivated shellfish in China, scallops are commonly distributed alive, while certain parts are distributed in forms of processed products centering on the adductor muscle [10]; under such circumstances, more and more scientific research personnel work on the hot research direction of the parameters of the scallop shelling process and how to industrialize the production.

The adductor muscle of scallops is the key part to connect the shell and control the opening and closing of the shell. The adductor muscle exerts a large force concentrated on the adductor muscle scar between the shells, which has posed a great problem for

the development of scallop shelling technology [11,12]. Therefore, the study of the structural changes of the adductor muscle and shell material at the position of the adductor muscle mark under ultra-high pressure can provide technical support for the subsequent elaboration of the ultra-high pressure (UHP) shelling mechanism and the development of intelligent equipment.

In recent years, the research on the connection mechanism and interface structure characteristics of the shell and shell meat has gradually attracted the attention of researchers. The main component of the closed shell muscle of scallops is protein, which belongs to the muscle tissue. The shell is composed of more than 95% of calcium carbonate ($CaCO_3$)crystals. The connection of these two levels can be regarded as a biological composite material of inorganic and organic matter. The connection structure between the shell and interface and the inner surface structure of shell are shown in Figure 1.

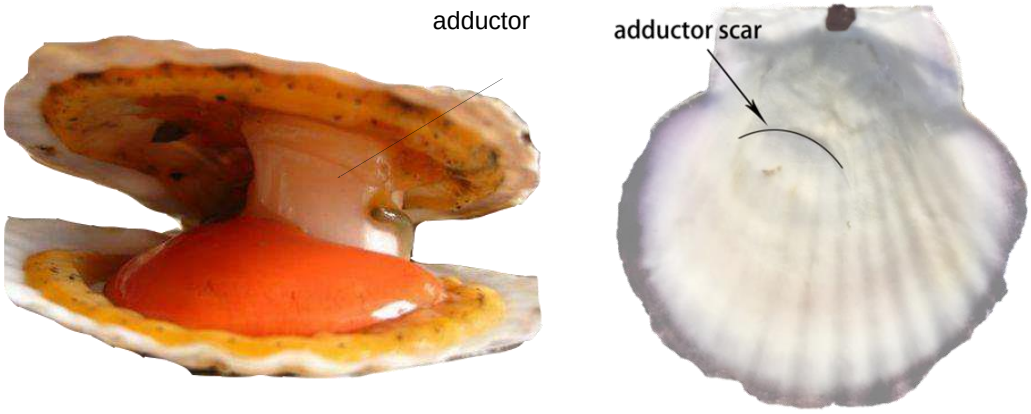

Figure 1. Connection structure between scallop shell and adductor muscle and internal surface structure of shell: (**a**) connection structure, and (**b**) internal surface structure.

Through research on the bonding interface of the shell and adductor muscle of shellfish food, previous researchers [13] consider shellfish food as a product combining mineral facies and organics. Meanwhile, interface observations show that the bonding interface between adductor muscle and interface fibers of the shell are connected with the shell at multiple points. The uniform distribution of pectinate muscle fibers reduces the stress concentration to a certain extent. Certain fibers of the adductor muscle are bonded to the shell by growth, and characterized by high strength. Moreover, based on research on structural characteristics of the adductor muscle interface, prior research found that there was an organic plasma membrane between the posterior obturator muscle and the surface of the muscle prism layer of the Mediterranean mussel, and there was a fibrous material connection between the muscle tissue and the membrane, forming a muscle–membrane–shell connection system [14]. The results of a study on the microstructure of shells by Luping Zhao [15] from Zhejiang University showed that shells are a highly ordered natural nanocomposite composed of $CaCO_3$ crystals and organic matter. Organic membranes in the shell connect the muscles to the shell calcium carbonate crystals. To sum up, scallops connect shells on two sides through the adductor muscle, so that the elasticity disappears and the fiber extends as the protein of the scallop shell and adductor muscle denatures during the UHP [16–18]. Therefore, it is of great significance to analyze the structural changes of the adductor muscle and shell at the connection interface of scallops under the action of UHP to reveal the influence of the structure on mechanical properties and explain the shelling mechanism of scallop based on elastoplastic mechanics.

2. Materials and Methods

2.1. Experiment Materials

2.1.1. Experiment Raw Materials

The experiment uses bay scallops that are abundant in coastal regions in Liaoning as the research object. The scallops were purchased at the seafood market of Bohai University, Jinzhou, Liaoning. Constrained by the entrance diameter of the UHP chamber, scallops of moderate and similar size were selected, with an average weight of 48 $\pm$ 5 g and the longest axis diameter of about 97 $\pm$ 5 mm.

2.1.2. Sample Pretreatment and Experimental Equipment

The scallops whose surfaces had been cleaned were put into a packaging bag made of polyethylene (PE), and 2% dilute salt water was injected into the packaging bags in order to distribute the pressure evenly; 100, 200, and 300 MPa were applied to the pretreated samples, respectively, and the muscle fibers and shell surface substances at the muscle scars of the shell were taken after UHP treatment. The pretreated sample was treated according to the requirements, and 2.5% glutaraldehyde solution, 0.2 mol/L phosphate buffer solution, ethanol and other regents were used after the sample treatment process. Ultra-high voltage equipment, a field emission scanning electron microscope, a Raman spectrum analyzer, and additional experimental equipment such as a Fourier-transform infrared spectrometer and a freeze dryer were used for our research.

2.2. Experiment Methods

2.2.1. Raman Spectrum Analysis

The adductor muscle of scallop was taken after ultra-high pressure treatment 1 mm above the connection interface and the isolated adductor muscle tissue of the shell was used as the sample. The excitation wavelength of 515.4 nm was set, and the slit was set at 200 μm. The Raman spectrum analyzer with a power of 129 mW and an exposure time of 60 s was used for three determinations [19], and the average value of the three results was taken to draw the Raman spectrum. The processed data were fitted by peaks to obtain the changes of the characteristic functional groups of the protein in the interface adductor muscle of the scallop treated by ultra-high pressure, and the mass fraction of the secondary structure of the protein was calculated.

2.2.2. Scanning Electron Microscopy Analysis

The adductor muscle at the contact surface of the scallop after ultra-high pressure treatment was fixed with 2.5% glutaraldehyde solution for 24 h, then rinsed with 0.2 mol/L phosphate buffer three times for 10 min each time, and then eluted with 50%, 60%, 70%, 80%, 90% and 100% ethanol gradient for 10 min, and then freeze-dried into powder. The surface of the shell was cleaned with deionized water for ultrasonic treatment, and the treated and dried adductor muscle and shell samples were observed and imaged at 20 thousand magnification after ion gradient gold plating.

2.2.3. Fourier-Transform Infrared Spectrum Analysis

We scraped the surface of the closed shell scar of the scallop shell treated by ultra-high pressure, and ground the powder in an agate mortar to obtain $\Phi \leq 200$ mesh powder samples. This was mixed with refined potassium bromide powder in a 1:100 ratio in the mortar, put into the mold to make a tablet, put in the Fourier-transform infrared spectrometer, with the scanning range of the spectrometer set to 400–4000 wave/cm, and the scanning frequency to 4 wave/cm, and scanned each sample 32 times to obtain the infrared spectrum of the shell, and analyze the spectral data obtained [20].

3. Results

3.1. Impacts on the Adductor Muscle Structure at the Bonding Interface of Scallops Produced by Ultra-High Pressure

Since scallops connect with the shell directly through the main muscle tissue, that is, the adductor muscle, it is required to break the connection between the shell and the adductor muscle to shell scallops. Therefore, the change of structure and characteristics of the adductor muscle is of extremely important significance for shelling scallops under ultra-high pressure. A great number of studies have shown that the adductor muscle mainly consists of fibrillin and a small amount of collagen. The protein denatures under ultra-high pressure. To this end, through analyzing the adductor muscle protein structure of scallops processed under UHP with Raman spectrum, we can obtain the change rule of adductor muscle elasticity under UHP and the influence of the scallop shucking mechanism, which lays a certain foundation for in-depth analysis of the scallop shucking mechanism.

Effect on the Structure of Adductor Muscle Interface

Raman Spectrum Analysis

Separate shells and adductor muscles of scallops were processed under different ultra-high pressures. According to the sample requirements of the Raman spectrum analyzer, we first cut the adductor muscle of the shell, then tested the adductor muscle at the interface position, and finally obtained the Raman spectrum data of the adductor muscle under different experimental pressure conditions. The Raman spectrum of adductor muscle changes at the interface under different experimental pressure is as shown in Figure 1.

Figure 2 shows that 11 characteristic peaks emerging in the Raman spectra of the adductor muscle at the bonding surface of scallops obtained under different UHP are mainly concentrated in two bands. The first is commonly known as the fingerprint area, the 500~1800 wave/cm, which mainly reflects the micro-environmental changes of amino acid residues existing in the adductor muscle and the spatial conformation of the protein. Ten characteristic peaks emerge in this band of the Raman spectra. Another characteristic peak refers to the hydro-carbon bond (-C-H-) stretching vibration area of 2800~3050 wave/cm [21]. Through analyzing parameters such as peak shapes and peak intensity of the characteristic peaks of the adductor muscle at the interface in the two Raman bands, the effects on structural changes of the adductor muscle at the interface brought by different ultra-high pressure may be explained.

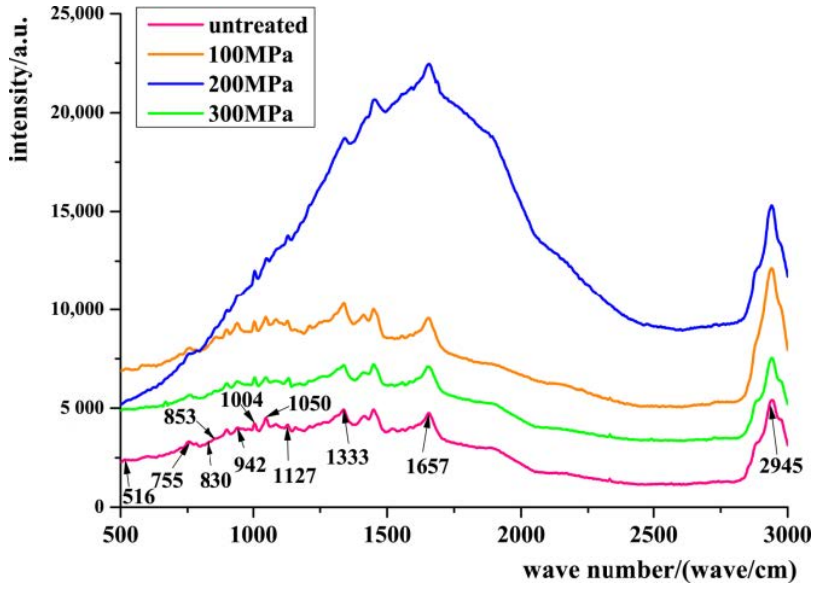

Figure 2. Raman spectra of structural changes of organic materials in adductor muscle under different experimental pressures.

Figure 2 shows that the adductor muscle of scallops at the interface has an obvious peak in the amide III bands (1335 wave/cm) and the amide I band (1657 wave/cm) [22–24]. Both the characteristic peak intensities increase firstly and then decrease as the experimental pressure increases. The band at these two positions mainly manifests the vibration situation of the protein backbone [25], including the nitrogen–hydrogen bond (-N-H-) in-plane bending vibration, carbon–nitrogen bond (-C-N-) vibration stretching, carbon–oxygen bond (-C=O-) in-plane bending vibration, carbon–carbon bond (-C-C-) stretching vibration, and other vibration forms. Meanwhile, as pressure increases, the two peaks maintain their position while the peak intensity changes. The peak intensity increases under an experimental pressure of 100 MPa, which demonstrates that the α-helix of the protein increases for the hydrogen bonds formed, promoted by the experiment pressure of 100 MPa.

However, as the pressure increases continuously, the peak intensity decreases, which demonstrates that hydrogen bonds are opened and the helix is extended and transformed into the β-sheet when the α-helix is affected under the pressure. Therefore, it can be concluded that the UHP changes hydrogen bonds existing between protein molecules, and triggers the secondary structure change of the protein, so that the original spatial conformation is damaged. Moreover, a C-C stretching vibration absorption peak is shown at 942 wave/cm.

As shown in Figure 1, the peak intensity at this point increases significantly under the pressure compared with the unprocessed adductor muscle of scallops. Meanwhile, it decreases as the pressure increases. The absorption peak at this point manifests another very important characteristic peak of α-helix in the Raman spectrum. The peak intensity change rules manifest that α-helix is sensitive to pressure changes. Low pressure promotes the formation of α-helix, and high pressure reduces α-helix by damaging the hydrogen bonds.

Changes in Secondary Structure

In the Raman spectrum, rich information related to the secondary structure of the protein [26] is shown in 1600–1700 wave/cm, the amide I band, including C=O stretching vibrations between protein molecules, C-N stretching vibrations within peptide chain, and in-plane bending vibration of C-N and N-H. Meanwhile, changes occurring to the secondary structure will also significantly affect the shelling of scallops. Current analysis results obtained related to the Raman spectrum show that the secondary structure quantification and backbone conformation of protein are closely connected with the band information of the Raman spectrum in the amide I band. Under ultra-high pressure, the complexity that changes the hydrogen bond between polypeptide molecules changes the protein molecular conformation, as well as the Raman spectrum information in the amide I band [27]. Therefore, it plays a vital role in analyzing the secondary structure of the protein following the Raman spectrum for research on the protein conformation and shelling mechanism of scallops. The Raman spectra obtained under different experimental conditions were analyzed by deconvolution method and second derivative solution method to analyze the Raman spectra of the amide I band at the interface of adductor proteins. The curve of peak segmentation and iterative fitting is shown in Figure 3.

Figure 3 shows the peak split and iterative fitting curve of the adductor muscle at the interface of unprocessed scallops and scallops processed under experimental pressures of 100, 200, and 300 MPa in the amide I band. By comparing the peak area corresponding to the α-helix, β-sheet, β-turn, and random coil in the protein, the relative content of each secondary structure covered by the adductor muscle protein at the interface of scallops was obtained. The relative content of the main secondary structure of the protein under different experimental pressure is as shown in Figure 4.

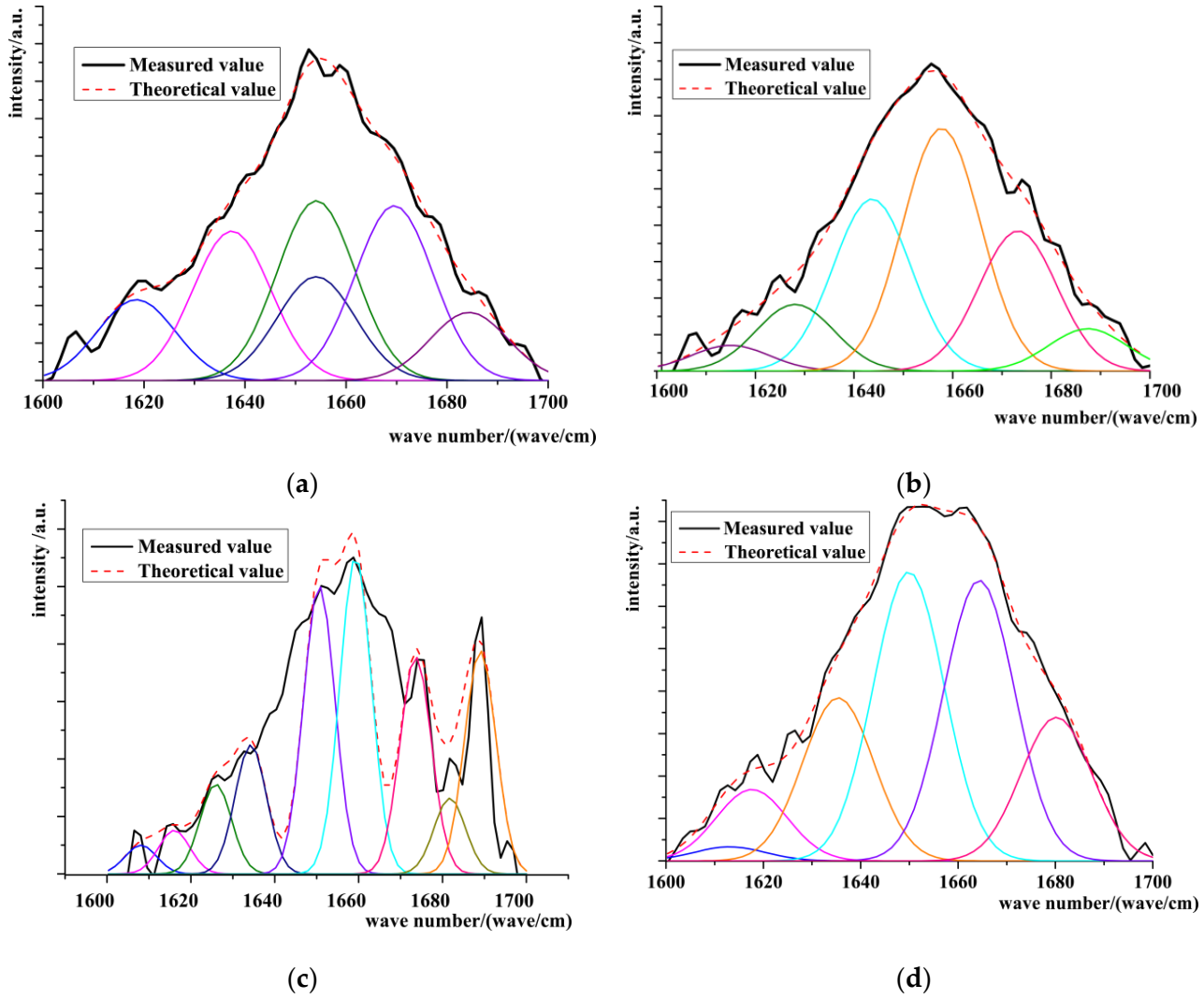

Figure 3. Protein amide I discrimination peak and iterative fitting curve of scallop interface adductor muscle under pressure. (**a**) Untreated; (**b**) 100 MPa; (**c**) 200 MPa; (**d**) 300 MPa.

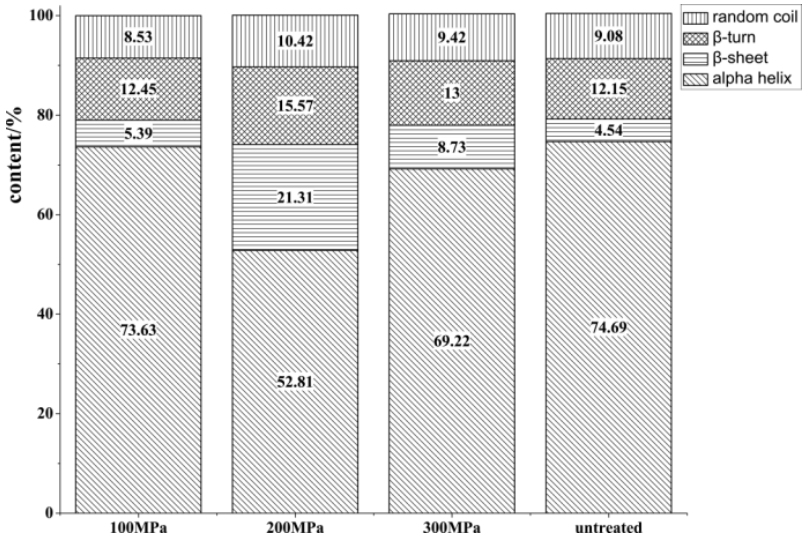

Figure 4. Changes of protein secondary structure of adductor muscle at scallop interface under ultra-high pressure.

Figure 4 shows that α-helix is the main component constituting the secondary structure of scallops' adductor muscles. Compared with the adductor muscle of unprocessed scallops, the content of α-helix reduces to a certain extent as pressure on scallops increases. Especially when the pressure reaches 200 MPa, the α-helix structure reaches its minimum content of 52.81%. Hydrogen bonds between protein molecules are damaged when the pressure reaches an ultra-high level of 200 MPa. As a result, the content of the α-helix structure decreases. However, the content of the α-helix structure increases again to 69.22% when the pressure increases to 300 MPa. This increases the content of α-helical structure, which is consistent with the results of Raman spectroscopy. Under ultra-high pressure, the content of the β-sheet is negatively correlated with the content of the α-helical structure. Such a situation may be affected by the re-production of hydrogen bonds for reversible changes after the UHP and pressure relief process.

As pressure increases the content of β-turn increases firstly and then decreases. Meanwhile, as the pressure reaches 200 MPa, the content of β-turn reaches 15.57% of the highest content. However, when the pressure reaches 300 MPa, the content of the β-turn structure decreases slightly, indicating that protein molecular polypeptide chains have formed more spatial conformations of 180° rotation under the experiment pressure, which changes the spatial conformation of adductor muscle protein at the interface of scallops [28,29].

Under an experimental pressure of 100 MPa, the content of random coil reduces by 6.06% to 8.53%, which indicates that under such an experimental condition, the protein shows a more regular structure instead of denaturing. However, when the pressure increases to 200 MPa, the content of the random coil experiences an obvious change, that is, increases to 10.42%, which indicates that more regular structures existing in the protein have transformed into a disordered and crumbly peptide chain, resulting in a decrease in protein activity and increase in solubility. In addition, when the experiment pressure increases to 300 MPa, the content of the random coil slightly drops to 9.41%. The possible reason is that the protein structure undergoes a reversible change during the pressure relief process, which promotes the formation of new hydrogen bonds in the original crumbly peptide chain, and equips the protein with a new regular structure [30,31]. Therefore, it is concluded that the protein becomes the most sensitive when the experiment pressure reaches 200 MPa, under which the protein denatures significantly.

Scanning Electron Microscopy Analysis

To better research the effects on the adductor muscle at the interface of scallops produced by different UHP, the adductor muscle morphology at the interface of unprocessed scallops and scallops processed under different experimental pressures were scanned and analyzed. The results are as shown in Figure 5.

Figure 5 shows that the adductor muscle at the interface of unprocessed scallops manifests a relatively continuous and complete even fibrous dispersion. Meanwhile, the fibers are basically distributed parallel to each other, and characterized by a certain regularity in shape. When the experiment pressure reaches 100 MPa, no huge changes are found in the adductor muscle fibers of scallops and in those of unprocessed scallops. However, the fiber distribution is slightly messy. As the experiment pressure increases to 200 MPa, a small amount of spherical loose structure emerges on the protein fiber surface, and the adductor muscle fibers are intricately distributed. As the experiment pressure continues to increase to 300 MPa, the protein fiber shortens, the fiber becomes thick and uneven, and the original columnar cross-section fibers become flat sheet in cross-section. The possibility is that the α-helix structure is damaged and hydrogen bonds are opened under the experiment pressure, so that the helix is extended and transformed into the β-sheet structure.

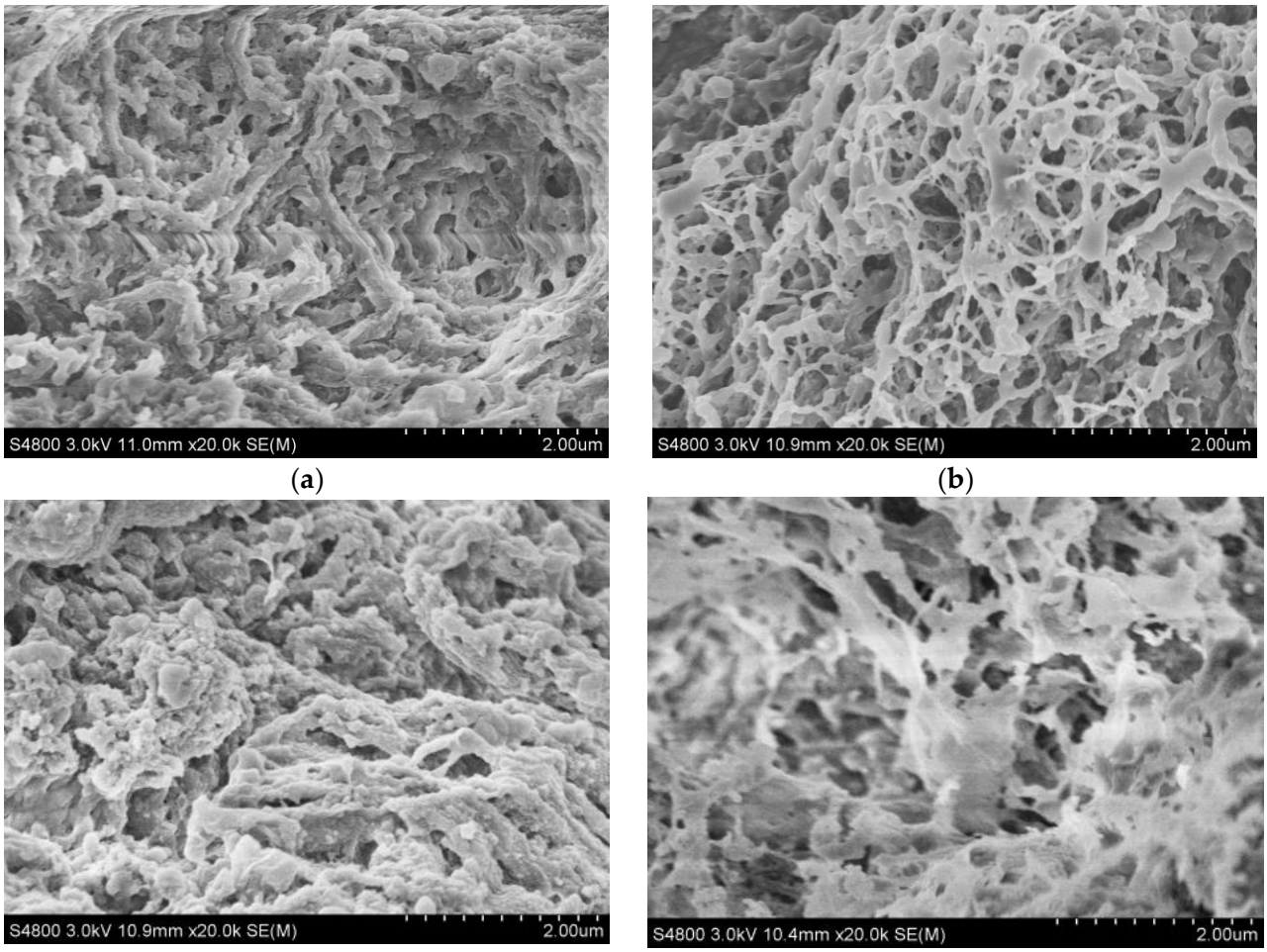

Figure 5. Fiber diagrams of interface adductor muscle under different experimental conditions. (**a**) Untreated; (**b**) 100 MPa; (**c**) 200 MPa; (**d**) 300 MPa.

3.2. Structural Changes of Organic–Inorganic Composites at the Interface of Scallop Shells under Ultra-High Pessure

3.2.1. Infrared Spectroscopic Analysis

In order to analyze the structural changes of the inorganic and organic matter in the scallop interface shell under the action of ultra-high pressure, the inner surface materials of the scallop closed shell muscle scar were scraped under different treatment conditions to make powder. After the powder was extracted and made into tablets, Fourier-transform infrared spectrum analysis was carried out. The Fourier-transform infrared spectra under different ultra-high pressure conditions were obtained as shown in Figure 6.

Figure 6 shows that different changes are found in the FTIR spectrum intensity of scallop shells. FTIR analysis found eight obvious characteristic peaks in the infrared spectra of the scallop shells. Previous studies found that the free-state CO_3^{2-} anion refers to the symmetrical regular triangle configuration of the D3h point group [32–34]. Moreover, four vibration peaks can be observed in the infrared spectrum, including the anti-symmetric stretching vibration v_3 at 1473 wave/cm, symmetric stretching vibration v_1 at 1074 wave/cm, out-of-plane bending vibration v_2 at 864 wave/cm, and shear-type in-plane bending vibration v_4 at 707 wave/cm, which indicates that the main inorganic phase of scallop shells consists of calcium carbonate crystals [35,36]. In addition, the v_3 characteristic peak at 1473 wave/cm is the widest in shape and strongest in intensity. Compared with absorption peaks at other positions, it is less sharp, which indicates that the absorption peak at 1473 wave/cm is probably generated by the overlapped vibration

of both organic and inorganic substances [37]. The v_2 vibration peak at 864 wave/cm is relatively sharp, while the v_4 at 707 wave/cm and v_1 at 1074 wave/cm, characteristic peaks are characterized by relatively small values and peak widths. Under different ultra-high pressures, the number and position of infrared spectral characteristic peaks of scallop shells do not change, which indicates that the structure of the scallop shell remains intact under ultr-high pressures. However, the same characteristic peak has changed in absorption intensity to a certain extent.

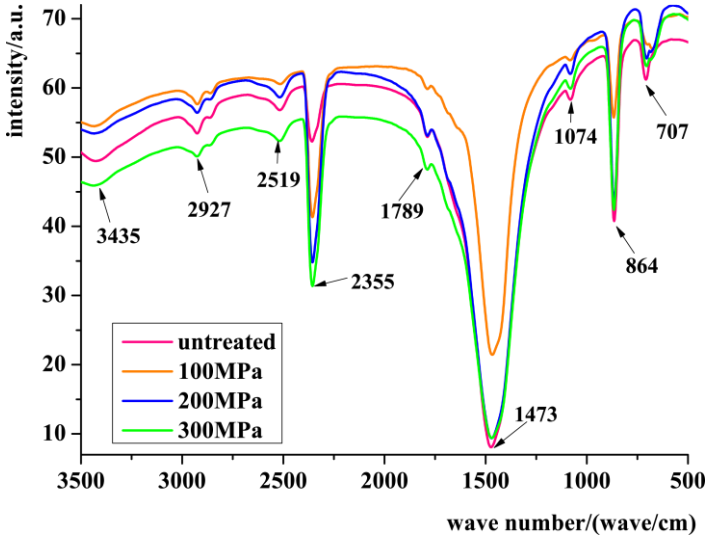

Figure 6. Structural changes of shell composites at the interface of scallops under ultra-high pressure.

Except for the four obvious peaks possessed by calcium carbonate crystals that are manifested in the infrared spectrum of scallop shells, the emergence of protein and chitin characteristics peaks at 3435, 2927, 2519, 2355, and 1789 wave/cm indicates that a small number of organic substances exist in scallop shells. Each infrared characteristic peak, functional groups, and corresponding structures [38] are as shown in Table 1.

Table 1. Comparison table of infrared spectrum characteristic peak and corresponding structure.

Serial Number	The Wavelength of Characteristic Peak/Wave/cm	Functional Group	Corresponding Structure
1	3435	N-H	Stretching vibration
2	2927	$-CH_3-$	Symmetric stretching vibration of anti $-CH_3-$
3	2519	-SH-	Stretching vibration of -SH-
4	2355	O=C=O	Antisymmetric stretching vibration
5	1789	C=O	Stretching vibration of C=O
6	1473	O=C=O	Antisymmetric stretching vibration of CO_3^{2-}
7	1074	O=C=O	Symmetric stretching vibration of CO_3^{2-}
8	864	O=C=O	Out-of-plane bending vibration of CO_3^{2-}
9	707	O=C=O	In-plane bending vibration of CO_3^{2-}

The two absorption peaks shown at 3435 and 2927 wave/cm in the infrared spectrum in Figure 5 represent N-H stretching vibration and $-CH_3$ anti-symmetric stretching vibration. Such a fact indicates that scallop shells also contain a small amount of protein except for calcium carbonate. Moreover, the other two absorption peaks representing N-H stretching vibration and -SH- anti-symmetric stretching appear at 2927 and 2519 wave/cm. The possible causes are that these two peaks are triggered by the small amount of chitin contained in the shell [39]. As the experiment conditions change, the absorption peak keeps intact, but the intensity of absorption peaks undergoes significant changes as processing conditions change. Figure 5 shows that when the experiment pressure reaches 100 MPa,

the intensity of the absorption peaks changes greatly, especially the v_3 characteristic peak at 1473 wave/cm and the v_2 absorption peak at 864 wave/cm, which shows that CO_3^{2-} out-of-plane bending vibration and anti-symmetric stretching vibration [40–44] undergo the greatest changes, while the intensity of the absorption peaks basically keeps intact under experimental pressures of 200 and 300 MPa. Meanwhile, the organic substances contained in scallop shells also changed to different degrees. As pressure increases, the intensity of the characteristic peak that represents the cumulative double-bond vibration at 2355 wave/cm increases accordingly. The increase in absorption peak intensity implies corresponding increases in vibration intensity. Furthermore, the fact that no obvious changes are found in the absorption peak intensity at other positions indicates that the UHP only brings a little effect on the polarity of matrix protein molecules contained in scallop shells [45].

To sum up, the peak shape, half-width of the peak, and peak intensity shown in the Fourier-transform infrared spectra of the shell at the scallop interface can be significantly changed under different experimental pressures and dwell times. Such a fact is probably affected by changes that occurred in the interaction between the aragonite calcium carbonate crystals and organic substances in the shell, as well as changes that occurred in the inorganic phase under UHP conditions. As the pressure reaches 300 MPa, the characteristic map of the organic phase exists continuously, as well as the organic substances, which indicates that the interaction between the inorganic–organic phase in the shell is characterized by a certain stability and high-pressure resistance.

3.2.2. Secondary Structure Changes

Scallop shells also contain small amounts of organic matter, mainly proteins and matrix proteins, which, although not high in the shell, play a regulatory role in the formation and growth of $CaCO_3$ crystals and also give the shell excellent mechanical properties [46]. The "sandwich" formed by matrix proteins in the shells with the matrix proteins, and the "sandwich" lattice structure formed by titin and matrix proteins in shells form the basis for the structural framework of shells [47]. Matrix proteins in shells can be divided into soluble matrix proteins and insoluble matrix proteins, and through analysis, the effect of ultra-high pressure on the polarity of protein molecules is more obvious, which can improve the solubility of proteins and thus combine with inorganic substances in calcium carbonate crystals to form new hydrogen bonds, thus controlling the directional growth and conversion of $CaCO_3$ crystals in scallop shells, while the insoluble proteins become the framework of shells.

To further attribute and analyze the FTIR spectrograms of scallop shells, we refer to the method of Surewica et al. (2012) [48]. C=O vibrational stretching, which is sensitive to changes in protein secondary structure, occurs at 1689 wave/cm in scallop shells, therefore, by using deconvolution and second-order derivative methods for subpeaks in the amide I band and fitting them with Gauss functions, it is possible to calculate the area of each subpeak and the content of protein secondary structures in scallop shells. According to the results of the study on the attribution of each subpeak in the absorption band of protein amide I, 1650–1658 wave/cm is the absorption band of α-helix, 1610–1640 wave/cm is β-folding, 1660–1700 wave/cm is β-turning, 1640–1650 wave/cm is irregularly curled [49]. Based on the experimentally measured infrared spectra of the scallop–shell interface, the infrared spectral data under different UHP treatment conditions were analyzed, and the changes of the organic matter secondary structure of the scallop–shell interface under UHP were obtained as shown in Figure 7.

As can be seen from Figure 7, the content of β-fold and irregular curl in the shells increased, while the content of α-helix and β-turn decreased, compared with the untreated specimens. When the experimental pressure increased, the contents of α-helix, β-fold and irregular curl in scallop shells increased and then decreased, while the contents of β-turn angle decreased and then increased, which was related to the change of vibrational intensity of shell protein functional groups under the action of ultra-high pressure. When the pressure was 100 MPa, the content of α-helix decreased by 9.72%, the content of β-fold

increased by 11.93%, and the irregular curl increased by 7.21%; when the pressure increased to 200 MPa, the content of α-helix, β-fold, and β-turn angle structures also increased; when the pressure increased to 300 MPa, the ultra-high pressure force changed the molecular force between peptide chains, so the α -helix and β-fold structures were destroyed, and the loose peptide chain structure continued to increase. In conclusion, compared with the untreated scallop shells, the decrease of the α-helical structure and the increase of the β-turned structure of the proteins on the inner surface of the interfacial shells under ultra-high pressure made the structure of protein molecules more stretchy, which could improve the interaction between organic matter and inorganic matter and improve the compatibility of molecules.

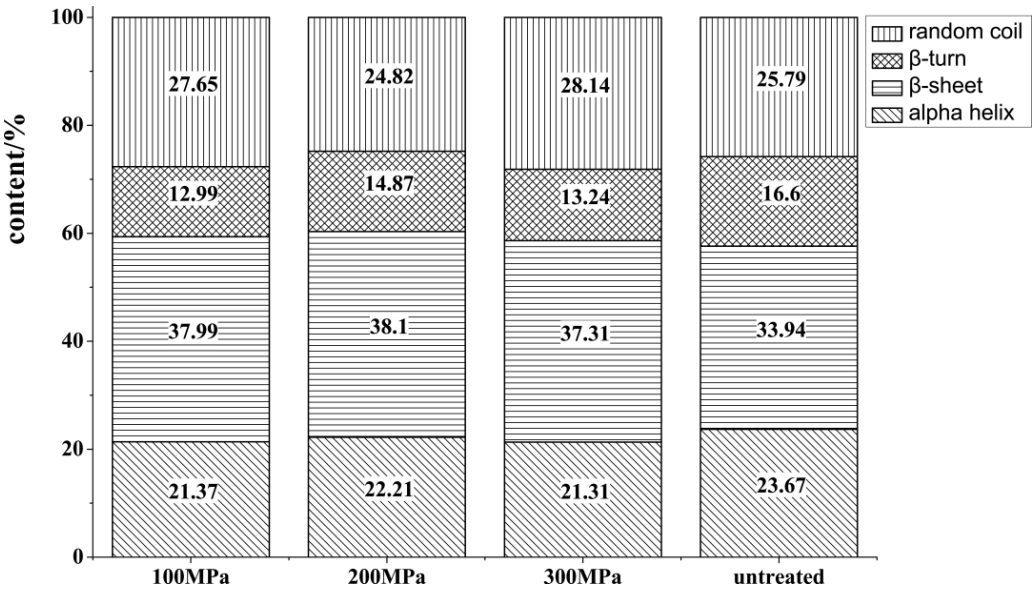

Figure 7. Changes in the secondary structure mass fraction of organic matter in scallop shells under ultra-high pressure.

3.2.3. Micro-Structure Analysis of the Inner Surface

After removing the adductor muscle from the shells of scallops processed under different ultra-high pressures, the inner surface of the scallop shells was cleaned with deionized water and ultrasound to ensure the inner surface cleanness of the scallops. Meanwhile, once gold plating and conductive measurements were carried out on the inner surface of scallops, samples were observed under a field emission scanning electron microscope. Next, these were compared with the inner surface structure of unprocessed scallops to obtain the micro-structure of the inner surface of the scallop under different experiment conditions, which is as shown in Figure 8.

Figure 8a shows that the scallop shell is not that smooth due to the scattered uneven structures. These structures may refer to the organic membrane structure used to connect the shell with the adductor muscle. Meanwhile, such an uneven surface has increased the surface friction for the connection between the shell and the adductor muscle, and increased the interface strength. Moreover, a small number of small holes with a diameter of about 0.7 μm are macroscopic on the inner surface of the shell, which will be left over when the adductor muscle fibers that grow inside the shell are pulled out. These small holes have decentralized the connection stress between the shell and the adductor muscle fibers to a certain extent, by which means stress concentration is avoided. As a result, the connection strength between the scallop shell and the adductor muscle interface is greatly enhanced.

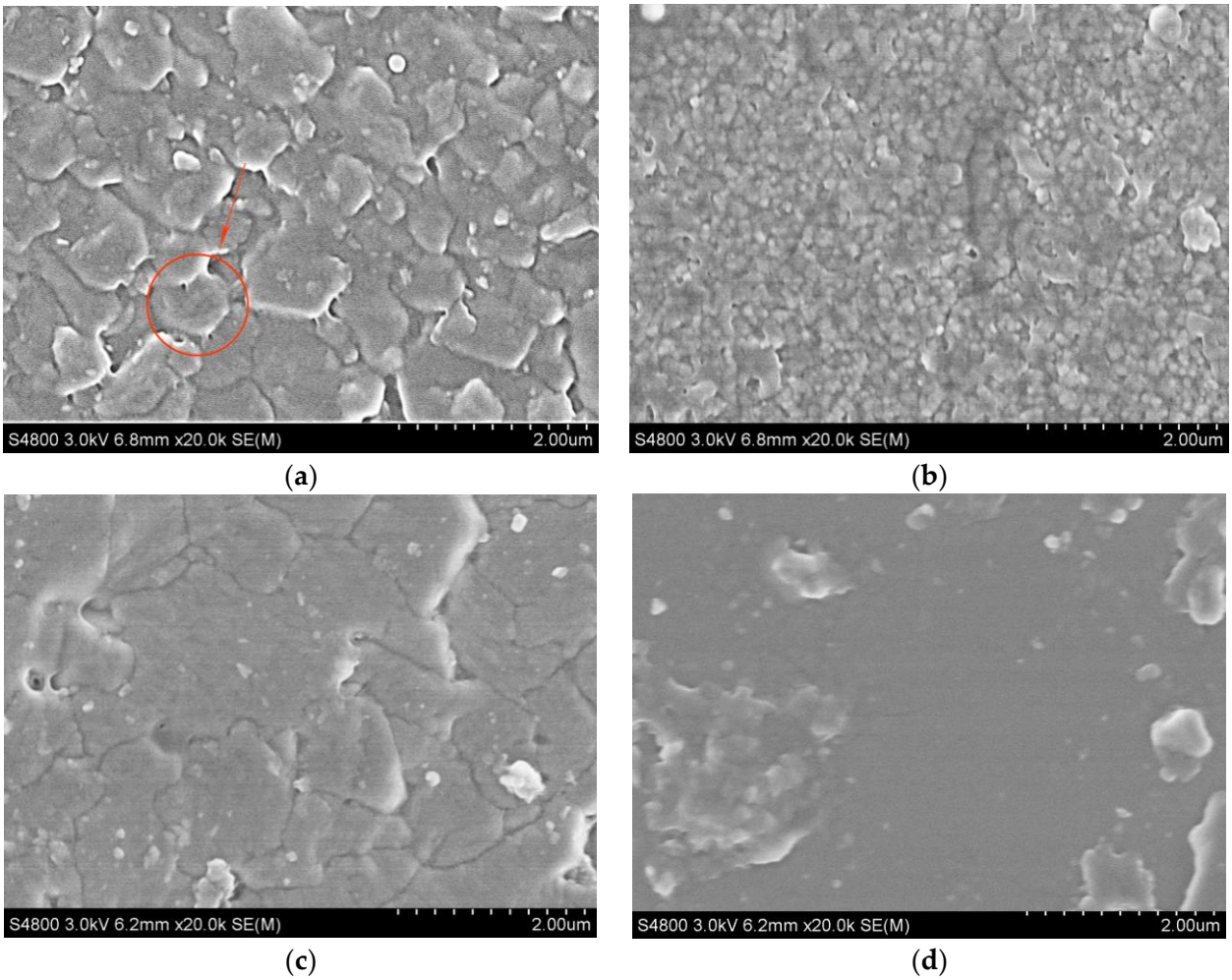

Figure 8. Inner surface state of scallop–shell interface under different experimental conditions. (**a**) Untreated; (**b**) 100 MPa; (**c**) 200 MPa; (**d**) 300 MPa.

Figure 8b–d show that when the pressure reaches 100 MPa, the concave–convex structure units scattered on the inner surface of the shell become smaller compared with those of unprocessed scallops. Meanwhile, as the pressure continues to increase, the original continuous, uneven structures scattered on the inner surface of the shell concentrate gradually to form an obvious discontinuous blocky structure. The possible reason is that under ultra-high pressure, the protein of the organic membrane existing on the inner surface of the shell denatures, which brought changes to the connecting medium that is used to connect the adductor muscle with the shell. Meanwhile, as the pressure continues to increase, the pores existing on the inner surface of the scallop shell fade, which may possibly be caused by the protein deformation under high-pressure conditions, so that the fluidity increases. As a result, the originally remaining small pores are filled. In conclusion, changes occurring to the organic membrane protein structure that connects the adductor muscle and the shells change the inner surface morphology of the shells, which definitely changes the interface bonding force, and affects the shelling effect of scallops.

To sum up, under different UHP conditions, the inner surface structure of the shell at the adductor muscle undergoes quite significant changes, especially in the organic membrane structure of the inner surface of the shell that exists between the inorganic and organic phases, because changes that occurred to this transparent organic membrane structure change the mechanical characteristics of the scallop interface and weaken the bonding force. As the protein denaturation of the organic membrane intensifies, the originally evenly distributed stress on the interface is gradually concentrated. As a result,

stress concentration emerges at one or even several parts. As more stress concentrations appear, the more significant the effect grows, and the greater the interface failure expands.

4. Discussion and Conclusions

4.1. Contrasts to Previous Studies

The paper investigated the structural changes of the closed-shell muscle and shell at the scallop linkage interface under different ultra-high pressures, and the results showed that the action of ultra-high pressure promoted the formation of protein intermolecular forces, and the intensity of the characteristic peak of the main chain of the closed-shell muscle protein increased, and the organic matter was denatured under the 200 MPa experiment, but a reversible reaction occurred at 300 MPa, and some of the hydrogen bonds were repaired, and the intensity of the characteristic peak converged to that of the untreated closed-shell muscle. This result is consistent with the subsequent secondary structure calculations and microstructural observations, and is in agreement with the results obtained by Choi and Ma (2007) [50] and Zhang et al. (2019) [27]. Under ultra-high pressure, the $CaCO_3$ crystal structure of the scallop–shell interface changed relatively little, and the organic matter on the inner surface of the shell was denatured under ultra-high pressure, and combined with the microstructure, and we found that the originally homogeneous stress was at the organic–inorganic interface. This trend is consistent with the change of protein structure under the action of ultra-high pressure.

4.2. Research Implications

According to the results of the study, the organic–inorganic composite interface structure of scallops changed under ultra-high pressure, which weakened the interfacial bonding force, and it is one of the effective ways to deshell the scallops, and it can protect the nutritional value and improve the texture of scallops. However, the energy consumption, low efficiency and high cost of UHP processing have limited the upscaling of UHP processing. From the interface structure of composite materials, we can explore the interface failure caused by its mechanical properties, which can lay the foundation for the subsequent establishment of mathematical models and provide the basis for the development of intelligent equipment. The UHP technology can change the interaction force between inorganic and organic matter organisms, and has a greater fit in the research fields of toughening and mechanical property improvement of biocomposites, and human compatibility and mechanical properties of bionic organs. Therefore, the UHP technology can be applied not only to aquatic deshelling, but also to medical and biological research on the mechanical properties of inorganic–organic composites.

Author Contributions: Conceptualization, X.G.; methodology, N.X.; formal analysis, Y.Z.; data curation, D.L.; writing—original draft preparation, X.G.; writing—review and editing, Z.S.; supervision, Z.S.; project administration, J.C.; Manuscript correction and sentence correction, J.W.; funding acquisition, Z.S. All authors have read and agreed to the published version of the manuscript.

Funding: This research was funded by The 13th Five Year National Science and Technology Support Program (grant number 2016YFD0400301) and also funded by the food source-based functional active packaging discipline team of Northeast Agricultural University (grant number 54941112).

Institutional Review Board Statement: Not applicable.

Informed Consent Statement: Not applicable.

Data Availability Statement: The date presented in this study are available in this article.

Acknowledgments: The authors are grateful to Light Industry College of Harbin University of Commerce and Bohai University for providing the necessary facilities to carry out this research work. Authors express their sincere thanks to the reviewers for the valuable comments and suggestions on this manuscript.

Conflicts of Interest: The authors declare no conflict of interest.

References

1. Zhang, Y.J.; Zhan, S.M.; Cao, P.L.; Liu, N.; Chen, X.H.; Wang, Y.J.; Wang, C.B. The polypeptide in *Chlamys farreri* can protect human dermal fibroblasts from ultraviolet B damage. *Chin. J. Ocean Limn.* **2005**, *23*, 357–362. [CrossRef]
2. Fishery administration bureau of the ministry of agriculture and rural areas. In *China Fishery Statistical Yearbook of 2020*; China Agricultural Press: Beijing, China; pp. 1–50.
3. Wang, Z.X.; Li, Y.S. Shellfish food and blood lipid. *Foreign Med. Hyg. Vol.* **1995**, *6*, 338–340.
4. Li, W.Q.; Wang, J.; Sun, J.F.; Li, W.S. The nutrients analysis and evaluation of *argopectens irradia*. *Acta Nutr. Sin.* **2007**, *33*, 630–632.
5. Wang, L. On the nutritional value, biological activity and culture of scallop. *J. Mudanjiang Univ.* **2007**, *16*, 92–94.
6. Pham, H.; Shihoko, K.; Shin-Ichi, Y.; Ken-Ichi, O.; Koji, Y. Dietary effect of EPA rich and DHA rich fish oils on the immune function of rats. *Biol. Sci.* **2009**, *16*, 135–140. [CrossRef]
7. Huang, X.C.; Liu, H.H.; Su, X.R. Study on the content of fatty acids in gonads of seven species of economic shellfish. *Fish. Sci* **2005**, *8*, 20–22. [CrossRef]
8. Wang, X.J.; Liu, X.S.; Sun, K.; Yang, L.H.; Yao, M.Y.; Jiang, F.F. Extraction and analysis of nutritional components of *chlamys farreri*. *Food Sci.* **2007**, *28*, 271–275. [CrossRef]
9. Susan, D.I.; Arin, K.; Mark, A.F.; Megan, L.; Kevin, S. Gray meat in the atlantic sea scallop, *Placopecten magellanicus*, and the identification of a known pathogenic scallop apicomplexan. *J. Invert. Pathol.* **2016**, *141*, 66–75. [CrossRef]
10. Zhou, Y.L.; Zheng, Y.; Liu, H.H.; Yan, L.; Zheng, Y.; Liu, H.; Zhang, Q.; Song, Y.; Tian, Y.Y.; Liu, J.R. Activity and characteristics of superoxide dismutase in adductor muscle of live dry—Storaged yesso scallop *Patinopecten yessoensis*. *J. Dalian Ocean Univ.* **2018**, *33*, 651–657. [CrossRef]
11. Thomas, W.E. Understanding the counterrntuitive phenomenon of catch bonds. *Curr. Nanosci.* **2007**, *3*, 63–77. [CrossRef]
12. Weiss, I.M.; Lüke, F.; Eichner, N.; Guth, C.; Clausen-Schaumann, H. On the function of chitin synthase extracellular domains in biomineralization. *J. Srruct. Biol.* **2013**, *183*, 216–225. [CrossRef] [PubMed]
13. He, J.B.; Wen, S.L. Interface features of shell and closed-shell-muscle. *J. Inorg. Mater.* **1998**, *13*, 127–128. [CrossRef]
14. Liao, Z.; Sun, Q.; Jiang, Y.T. Molecular composition and mechanism of muscle-shell attachment of shellfish. *J. Zhejiang Ocean Univ. (Nat. Sci.)* **2018**, *37*, 313–319.
15. Zhao, L.P.; Xu, H.Z.; Chen, D.; Bao, L.F.; Fan, M.H.; Liao, Z. Microstructure and spectral analysis of *Mytilus* coruscus shell. *J. Zhejiang Univ. (Sci. Ed.)* **2015**, *42*, 339–346. [CrossRef]
16. Chen, Q.H.; Wen, L.H.; Chen, X.; Fang, X.B.; Ling, J.G.; Xuan, X.T. Effect of ultra-high pressure assisted shelling on biochemical characteristics and structure of myofifibrillar protein in *Patinopecten Yessoensis*. *Food Sci.* **2021**, *42*, 102–107. [CrossRef]
17. Benjakul, S.; Visessanguan, W.C.; Thongkaew, M.T. Comparative study on physicochemical changes of muscle proteins from some tropical fish during frozen storage. *Food Res. Int.* **2003**, *36*, 787–795. [CrossRef]
18. Zhang, P.X.; Zhou, X.F.; Fang, Y. Raman spectra of vegetables and fruits at two excitation wavelengths. *J. Light Scatt.* **2004**, *16*, 136–140. [CrossRef]
19. Michalczyk, M.; Surowka, K. Changes in protein fractions of rainbow trout (*Oncorhynchus mykiss*) gravads during production and storage. *Food Chem.* **2007**, *104*, 1006–1013. [CrossRef]
20. An, X.L.; Li, Q.Z.; Liu, H.P. FTIR study of the interaction between bovine serum albumins and cetyltrimethyl ammonium bromide. *J. Southwest Norm. Univ.* **2005**, *30*, 699–702.
21. Gao, W.H.; Ye, R.S.; Pan, T.T.; Zeng, X.A. Analysis of structural changes of surimi proteins during frozen storage by Raman spectroscopy. *Food Sci.* **2018**, *39*, 71–77. [CrossRef]
22. Chen, H.Y.; Han, M.Y. Raman spectroscopic study of the effects of microbial transglutaminase on heat-induced gelation of pork myofibrillar proteins and its relationship with textural characteristics. *Food Res. Int.* **2011**, *44*, 1514–1520. [CrossRef]
23. Bryant, R.N.; Pasteris, J.D.; Fike, D.A. Express: Variability in the raman spectrum of unpolished growth and fracture surfaces of pyrite due to laser heating and crystal orientation. *Appl. Spectrosc.* **2018**, *72*, 37. [CrossRef] [PubMed]
24. Herrero, A.M.; Cambero, M.I.; Ordóñez, J.A.; Hoza, L.D.L.; Carmona, P. Raman spectroscopy study of the structural effect of microbial transglutaminase on meat systems and its relationship with textural characteristics. *Food Chem.* **2008**, *109*, 25–32. [CrossRef] [PubMed]
25. Sun, W.Z.; Zhao, Q.Z.; Zhao, M.M.; Bao, Y.; Chun, C.; Jiao, Y.R. Structural evaluation of myofibrillar proteins during processing of Cantonese sausage by Raman spectroscopy. *J. Agric. Food Chem.* **2011**, *59*, 11070–11077. [CrossRef]
26. Zhang, T.; Li, Z.H.; Wang, Y.M.; Yong, X.; Chang, H.X. Effects of konjac glucomannan on heat-induced changes of physicochemical and structural properties of surimi gels. *Food Res. Int.* **2016**, *83*, 152–161. [CrossRef]
27. Zhang, D.K.; Zhang, H.E.; Zhu, Y.J.; Yang, J.P.; Lei, Y.S.; Yang, H.; Lou, Y.J. Effect of high hydrostatic pressure treatment on myofifibrillar protein structure of cultured large yellow croaker. *Food Sci.* **2019**, *40*, 61–67. [CrossRef]
28. Yang, H.; Lu, S.C.; Zhang, H.E.; Liu, L.J.; Qi, X.Y. Effects of high hydrostatic pressure processing on the flavor and quality of cultured Yellow croaker (*Pseudosciaena crocea*). *Food Sci.* **2014**, *35*, 244–249. [CrossRef]
29. Sano, T.; Ohno, T.; Otsuka-Fuchino, H.; Matsumoto, J.J.; Tsuchiya, T. Carp natural actomyosin: Thermal denaturation mechanism. *J. Food Sci.* **1994**, *59*, 1002–1008. [CrossRef]
30. Li, L.K.; Spector, A. Circular dichroism of beta-poly-L-lysine. *J. Am. Chem. Soc.* **1969**, *91*, 220–222. [CrossRef]
31. Herrero, M.A. Raman spectroscopy a promising technique for quality assessment of meat and fish: A review. *Food Chem.* **2008**, *107*, 1642–1651. [CrossRef]

32. Dauphin, Y. Infrared spectra and element al composition in recent biogenic calcites: Relationships between the υ4 band wave length and Sr and Mg concentrations. *Appl. Spectrom.* **1999**, *53*, 184–190. [CrossRef]
33. Baldauf, N.; Rndriguez, R.L.; YousefLuis, A.E.; Rodriguez, S.E. Effect of selective growth media on the differentiation of Salmonella enterica serovars by Fouriertransform mid-infrared spectroscopy. *J. Microbiol. Meth.* **2007**, *68*, 106–114. [CrossRef] [PubMed]
34. Gang, L.; Ji, L.; Ke, S.; Wang, S.; Chen, L.; Liu, Y.; Huang, Q. Composition, secondary structure, and self-assembly of oat protein isolate. *J. Agric. Food Chem.* **2009**, *57*, 4522–4558. [CrossRef]
35. Bao, L.F.; Gao, P.; Zhao, L.P. Microstructural characteristics and FTIR analysis of the shell from green mussel (*Perna canaliculus*). *J. Zhejiang Ocean Univ. (Nat. Sci.)* **2014**, *33*, 347–353. [CrossRef]
36. He, P.; Chen, J.X.; Su, M.; Han, J.; Cheng, K. Analysis of chemical composition and structure characteristics of shells. *Cecsc. J.* **2015**, *66*, 450–454. [CrossRef]
37. Liang, Y.; Zhao, J.; Wang, L. The fourier transform infrared spectroscopy(FT-IR) and thermal analysis of the mollusc shell. *J. Min. Pet. Sci.* **2007**, *27*, 12–16. [CrossRef]
38. Shi, Y.G.; Guo, Q.Q.; Yang, X.W.; Liu, X.F.; Wang, S.J.; Zhu, H.; Zhang, N. FTIR analysis on the structure of soybean—Casein protein complex. *Chin. J. Food* **2018**, *18*, 225–231. [CrossRef]
39. Ma, Y.F.; Qiao, L.; Feng, Q.L. Research progress on biomineralization mechanism of freshwater pearl. *J. Inorg. Mater.* **2012**, *8*, 109–116. [CrossRef]
40. Xie, C.F.; Qiu, T.Q.; Lu, H.Q.; Yang, L.S. Morphology variation of calciumcarbonate crystal irradiated by ultrasonic. *J. South China Univ. Technol. (Nat. Sci. Ed.)* **2007**, *35*, 62–66.
41. Lin, J.Y.; Ma, K.Y.; Bai, Z.Y.; Li, J.L. Molecular cloning and characterization of perlucin from the freshwater pearl mussel, Hyriposis cumingii. *Gene* **2013**, *526*, 210–216. [CrossRef]
42. Evans, J.S. "Tuning in" to mollusk shell nacre-and prismatic–associated protein terminal sequence. Implications for bio mineralization and the construction of high performance inorganic-organic composites. *Chem. Rev.* **2008**, *108*, 4455–4462. [CrossRef] [PubMed]
43. Zhao, Y.; Liu, X.L.; Wang, R.L.; Ma, Y.J.; Yang, J. Influence of storage microenvironment to the secondary structure in wheat proteins. *Cereals Oils* **2014**, *27*, 36–38.
44. Gao, L.L.; Wang, Z.Y.; Rao, W.L.; Cao, L.C.; Zhang, D.Q. Molecular interaction analysis between collagen and chitosan blend film based on infrared spectroscopy. *Trans. Chin. Soc. Agric. Eng.* **2018**, *34*, 285–291. [CrossRef]
45. Shi, L.; Xiong, G.Q.; Yin, T.; Ding, A.Z.; Li, X.; Wu, W.J.; Qiao, Y.; Liao, L.; Jiao, C.H.; Wang, L. Effects of ultra-high pressure treatment on the protein denaturation and water properties of red swamp crayfish (*Procambarus clarkia*). *LWT* **2020**, *133*, 110124. [CrossRef]
46. Stupp, S.I.; Braun, P.V. Molecular manipulation of microstructures: Biomaterials, ceramics, and semiconductors. *Nature* **1996**, *381*, 56–58. [CrossRef]
47. Ansboro, S.; Greiser, U.; Barry, F.; Murphy, M. Strategies for improved targeting of therapeutic cells: Implications for tissue repair. *Eur. Cells Mater.* **2012**, *23*, 310–318. [CrossRef]
48. Surewicz, W.K.; Mantsch, H.H. New insight into protein secondary structure in water from second-derivative amide I infrared spectra. *Biochim. Bilphys. Acta* **1988**, *952*, 115–130. [CrossRef]
49. Zhu, C.; Chen, L.H.; Zeng, X.Y.; Sun, Y.; Jiao, D.X.; Liu, M.H.; Zheng, M.Z.; Liu, J.S.; Liu, H.M. Effects of ultra high pressure-magnetic field treatment on protein properties and quality characteristics of stored shrimp (*Litopenaeus vannamei*). *LWT* **2022**, *170*, 114070. [CrossRef]
50. Choi, S.M.; Ma, C.Y. Structural characterization of globulin from common buckwheat (*Fagopyrum esculentum* Moench) using circular dichroism and Raman spectroscopy. *Food Chem.* **2007**, *102*, 150–160. [CrossRef]